Journal of the Korean Society for Nondestructive Testing
Vol. 27, No. 6 (2007. 12)

An Ultrasonic Measurement Model to Predict a Reflected Signal from Non-Linear Burning Surface of Solid Propellants

Sung-Jin Song*,†, Hak-Joon Kim*, Hyun-Taek Oh*, Sang Won Lee*,
Seung Hyun Song**, In-Chul Kim***, Ji-Chang Yoo*** and Jung Yong Jung***

Abstract While determination of the solid propellant burning rates by ultrasound, it has been reported that the frequent data scatters were caused by two major factors; 1) variation in the acoustical properties, and 2) non-linear burning of a solid propellant sample under investigation. This work is carried out for the purpose of investigating the effect of non-linear burning of solid propellant samples. Specifically, we propose an ultrasonic measurement model that can predict the reflections from solid propellant surfaces with non-linear burning by the combination of two ingredients; 1) a pulse-echo ultrasonic measurement model for a planar, circular reflector imbedded in the second medium in an immersion set-up, and 2) an efficient model of non-linear burning surfaces with a number of small, planar circles. Then, we demonstrate the capability of the proposed measurement model by simulation of the surface echo signals from four different burning surfaces that have been generated by the combination of two factors; the base shape (flat or paraboloidal) and the surface roughness (perfectly smooth or randomly rough). From the simulation presented here, we can confirm the fact that the non-linear burning of the propellant can cause the waveform change of the burning surface echo and the corresponding spectrum variation.

Keywords: Ultrasonic, Burning Rate, Solid Propellant, Non-Linear Burning Surface

1. Introduction

For reliable prediction and analysis of ballistic behavior of solid propellant rockets, it is necessary to accurately measure the burning rates of a solid propellant in a wide range of pressure. There have been proposed various methods to measure the burning rates of solid propellants. Among them, a strand burner method is widely adopted as a standard technique in industry (Sutton and Biblarz, 2001). However, it requires a number of measurements to determine the burning rates at many different pressures since the measurement is carried out under a constant pressure. To take care of such a difficulty, it has been proposed the ultrasonic techniques that can measure the burning rates as a function of pressure in a single test performed under a constant volume condition over many years ago (Frederick Jr. et al, 2000).

The principle of ultrasonic measurement of solid propellant burning rate is very simple. Fig. 1 a) schematically shows a typical ultrasonic measurement set-up where a normal beam ultrasonic transducer is attached to a solid couplant (usually made of resin) that is fixed

Received: October 12, 2007, Accepted: November 2, 2007. * School of Mechanical Engineering, Sungkyunkwan University, 300 Chunchun-dong, Jangan-gu, Suwon, Kyunggi-do 440-746, Korea, ** Department of Electrical Engineering, Iowa State University, Ames, Iowa 50010, USA, *** Agency for Defense Development, Jochiwongil 462, Yuseong, Daejeon, 305-152, Korea, † Corresponding author: sjsong@skku.edu

firmly to a solid propellant under interrogation. In this configuration, when ultrasonic pulse is excited by the transducer, the reflected signals are generated at two boundaries. (as shown in Fig. 1 b)); 1) the "interface echo" produced at the interfaceterms of time and cost.

As mentioned above, in the burning rate determination using ultrasound the ultrasonic time-of-flight information plays a key role so that accurate measurement of this parameter is a truly crucial task. To invoke this important information from ultrasonic signals, there have been proposed two approaches; 1) tracking the arrival time of a specific ultrasonic signal using dedicated hardware circuits (McQuade et al, 1998), and 2) acquiring the ultrasonic full waveforms to have post analysis. The first approach, however, requires carrying out three separate tests (a pre-test, a burning test and a post test) since the most hardware signal tracking circuits can search for only one peak at a time (Salvo et al, 1999). Thus, this approach is time and cost consuming. More recently, the second approach has been proposed with taking advantages of digital signal processing techniques. However, this approach usually requires a dedicated hardware and software system to acquire ultrasonic full waveforms and pressure data at a high enough speed. Recently, Song et al (2006) has developed such a system and applied it to measure the burning rates of various propellants with different burning characteristics (Song et al, 2007).

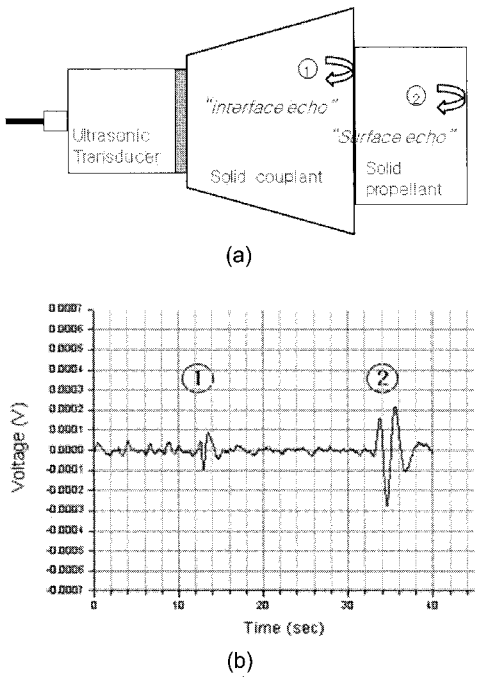

Fig. 1 Ultrasonic measurement of burning rates of a solid propellant sample; a) a typical measurement set-up and b) two reflected signals

In both approaches discussed above, however, the invoked time-of-flight information can be changed if the waveform of ultrasonic signal to be measured (i.e. the surface echo) varies. In fact, one can observe the surface echo waveform change in burning tests for almost all solid propellants. Obviously, this waveform change is not uniform through out the samples even in the same batch of a solid propellant. As a consequence, in the burning rate data determined by ultrasonic techniques there exist data scatters that can not be ignored. In fact, these data scatters quite often exceed a quality control limit (of 3.0 %) imposed by many propellant manufacturers. Thus, it is strongly desired to analyze the sources of this scattering for their proper reduction.

There would be two major factors that can cause the change of the surface echo waveform in the burning test; 1) variation in the acoustical properties, and 2) non-linear burning of a solid propellant sample under investigation. The acoustical properties of a solid propellant that should be considered include its velocity and attenuation. Very recently, Oh et al (2007) has investigated the effect of acoustical property variation on the invoked burning rate data scattering. They observed that the data scatter in burning rates had a proportional relation to in attenuation of a solid propellant under investigation. However, they did not analyze the effect of non-linear burning on the invoked burning rate data scatter. Therefore, it is necessary to have further investigation on the effect of non-linear burning of a solid propellant sample. In fact, the present study has been

performed with this task in mind.

As one may realize, there is no easy way to observe the morphology of burning surface during actual burning. Therefore, in the data analysis it is usually adopted an assumption of linear burning (which means that the burning surface of the solid propellant sample remains as a flat plane and moves along a straight line while maintaining the plane flat during entire burning). Obviously, the violation of this assumption during burning can produce the waveform change which would be one of the major sources of data scatter in ultrasonic measurement of burning rates. Unfortunately, however, it is not easy to examine the degree of violation from this assumption for a specific propellant sample since the real morphology is unknown. One potential way to detour such a difficulty is to rely on ultrasonic measurement models that can predict surface echo waveforms generated from solid propellants with non-linear burning surfaces. This paper proposes such an ultrasonic measurement model and demonstrates its capability of simulating the ultrasonic signals reflected from various non-linear burning surfaces.

2. Ultrasonic Measurement Model

Fig. 2 a) schematically represents an ultrasonic measurement set-up for acquiring a reflected signal from the burning surface of a solid propellant (i.e. the surface echo) with the parameters needed for constructing a measurement model. As shown in the figure, an ultrasonic normal beam transducer (with the center frequency of 0.5 MHz, and the diameter of 12.7 mm) is located at the origin of the Cartesian (x,y,z) coordinate system with radiating a bounded ultrasonic beam into the couplant located at the positive direction along z-axis. The interface between the couplant and the solid propellant is located at a plane with $z = h_1$, and the burning surface of the propellant at $z = h_2$, which is not a constant but a function of x and y coordinates. The densities of the couplant and the propellant are 1.29 g/cm^3 and 1.73 g/cm^3, respectively, and the longitudinal wave speeds of the couplant and the propellants are 2,500 m/s and 1920 m/s, respectively. The couplant is 42 mm long and about 40 mm in diameter, while the initial length of the propellant is 20 mm and its diameter is 28 mm.

$$V_R(\omega) = \sum_{n=1}^{N} v_n(\omega, x_n, y_n, z_n) \tag{1}$$

where $V_R(\omega)$ is the resultant reflection from the parabolidal burning surface with random roughness, and $v_n(\omega, x_n, y_n, z_n)$ is the reflection from a small circular reflector located at a point of (x_n, y_n, z_n). Obviously, N denotes the total number of small elementary circles. In this particular case, N = 367.

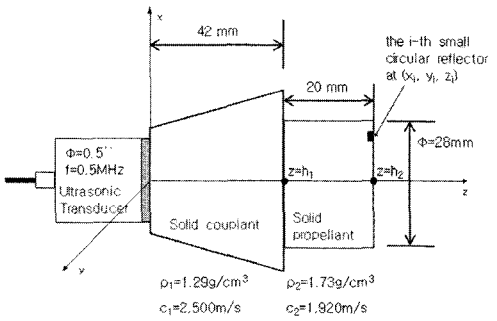

(a)

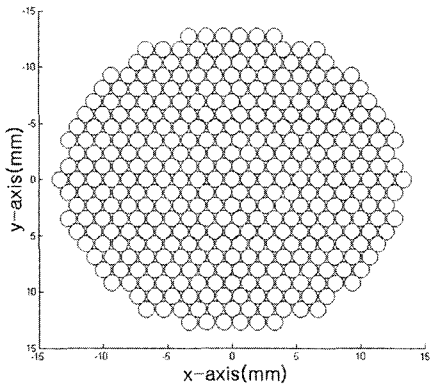

(b)

Fig. 2 Parameters for modeling ultrasonic measurement set-up; a) geometry of ultrasonic measurement of burning surface signal and b) division of burning surface with a number of small circles located at (x_i, y_i, z_i)

As shown in Fig. 2 a), the center of the transducer is located at the origin of the (x,y,z) coordinate system, while that of the n-th reflector is at the point having the coordinates of (x_n,y_n,z_n). Here, for the convenience of predicting the reflection from this elementary circle, we can have a following further simplification. In this ultrasonic testing configuration, a normal beam transducer radiates the longitudinal wave into the solid couplant and the beam propagated through the couplant has a normal incidence to the interface between the solid propellant without mode conversion. These measurement characteristics allow us to have an approximation of considering the solid couplant as an equivalent fluid medium. This simplification, in turn, makes it possible to adopt an ultrasonic measurement model that has been discussed in detail by Schmerr and Song (2007) for this particular problem. The model given by Schmerr and Song can be applied to a variety of more general problems (with curved interfaces, oblique incidences, pitch-catch set-ups and so on), however, it is ideally suited for the current problem under consideration.

The reflection from a circular, planar reflector can be given by eqn. (2) (Schmerr and Song, 2007).

$$v_\eta(\omega,x_n,y_n,z_n)= s(\omega)\left[\hat{v}(\omega,x_n,y_n,z_n)\right]^2 A_n(\omega)\left[\frac{4\pi\rho_2 c_2}{-ik_2 Z_r}\right] \quad (2)$$

where, $s(\omega)$ is the system function $\hat{v}(\omega,x_n,y_n,z_n)$ is the incident velocity field at the n-th point of (x_n,y_n,z_n), $A_n(\omega)$ is the far-field scattering amplitude of the n-th reflector, Z_r is the acoustic radiation impedance that can be approximated as $Z_r=\rho_1 c_1(\pi a^2)$ at high frequency, where a is the radius of the radiating transducer. Obviously, ρ_1 and ρ_2 are the densities of the couplant and the propellant, respectively, and c_1 and c_2 are the longitudinal wave speeds in the couplant and the propellant, respectively, while k_2 is the wavenumber in the propellant.

The incident velocity field, $\hat{v}(\omega,x_n,y_n,z_n)$ can be written as

$$\hat{v}(\omega,x_n,y_n,z_n)= \exp\left[-\alpha_1(\omega)h_1-\alpha_2(\omega)h_2\right] \left[v(\omega,x_n,y_n,z_n)/v_0(\omega)\right] \quad (3)$$

where h_1, h_2 are the distances the sound beam propagated in the couplant and the propellant, respectively, and $\alpha_1(\omega)$, $\alpha_2(\omega)$ are the frequency dependent attenuation coefficients for the longitudinal waves in the couplant and the propellant, respectively. $v(\omega,x_n,y_n,z_n)$ is the ideal velocity field (that can be observed if the media were lossless) at the n-th reflector, and v_0 is the normal velocity on the face of the transducer.

The ideal velocity at the n-th reflector in the propellant can be given by eqn. (4) in the multi-Gaussian beam model with 15 coefficients (Schmerr and Song, 2007).

$$v(\omega,x_n,y_n,z_n)= \sum_{r=1}^{15} T_{12}\frac{\sqrt{\det\left[M_2(h_2)\right]_r}}{\sqrt{\det\left[M_2(0)\right]_r}}\frac{\sqrt{\det\left[M_1(h_1)\right]_r}}{\sqrt{\det\left[M_1(0)\right]_r}}\left[V_1(0)\right]_r \cdot\exp\left[ik_1h_1+ik_2h_2+i\frac{k_1}{2}\mathbf{y}^{\mathrm{T}}\left[c_1M_2(h_2)\right]_r\mathbf{y}\right] \quad (4)$$

where, $\mathbf{y}^{\mathrm{T}}=(x_n,y_n)$ and

$$\left[V_1(0)\right]_r=A_r v_0$$
$$\left[M_1(0)\right]_r=\begin{bmatrix}\frac{iB_r}{c_1D_r} & 0\\ 0 & \frac{iB_r}{c_1D_r}\end{bmatrix} \quad (5)$$

where, A_r, B_r are the Hwang and Breazeale coefficients (Hwang and Breazeale, 1999), T_{12} is

the plane wave transmission coefficient based on a velocity ratio. The parameter $D_r = \frac{k_1 a^2}{2}$ is the Rayleigh distance, and k_1 is the wavenumber in the couplant.

In addition, the other matrices appeared in eqn. (4) can be written as follows in this case.

$$\left[M_1(h_1)\right]_r = \begin{bmatrix} \frac{1}{c_1(h_1 - iD_r/B_r)} & 0 \\ 0 & \frac{1}{c_1(h_1 - iD_r/B_r)} \end{bmatrix}$$

$$\left[M_2(0)\right]_r = \left[M_1(h_1)\right]_r$$

$$c_1\left[M_2(h_2)\right]_r = \begin{bmatrix} \frac{1}{(h_1 - iD_r/B_r) + h_2\frac{c_2}{c_1}} & 0 \\ 0 & \frac{1}{(h_1 - iD_r/B_r) + h_2\frac{c_2}{c_1}} \end{bmatrix} \quad (6)$$

The plane wave far-field scattering amplitude, $A_i(\omega)$, appeared in eqn. (2) is chosen to describe the scattered field from the small reflector in the propellant. Based on the Kirchhoff approximation, the far-field scattering amplitude for a small, circular, planar reflector can be given by eqn. (7) (Schmerr, 1988).

$$A_n(\omega) = \frac{ik_2 b^2}{2} \quad (7)$$

where, b is the radius of the circular reflector.

The system function, $s(\omega)$, appeared in eqn. (2) is usually computed by the deconvolution of an experimental signal obtained from an independent, reference reflector by a corresponding theoretical reference reflector model, as given by eqn. (8) (Schmerr and Song, 2007):

$$s(\omega) = \frac{1}{2}\frac{V_0(\omega)}{V_R(\omega)}W(\omega) \quad (8)$$

where, $V_0(\omega)$ is a measured voltage by the experiments, $V_R(\omega)$ is the calculated voltage by the theoretical reference model and $W(\omega)$ is the Wiener filter.

In the present study, however, the experimentally measured voltage in the time domain, $V_0(t)$, assumed to be given by eqn. (9). Then, the system function was simply assumed to be the frequency spectrum of this theoretical reference signal.

$$V_0(t) = \begin{cases} \left[1 - \cos\left(\frac{2\pi f}{3}t\right)\right]\cos(2\pi ft) & for \quad 0 \le t \le \frac{3.0}{f} \\ 0 & otherwise \end{cases} \quad (9)$$

Fig. 3 shows the theoretical front surface reflection signal in time domain and the system function, $s(\omega)$, determined to be used for the prediction of the surface echoes from various burning surfaces to be addressed in the next section.

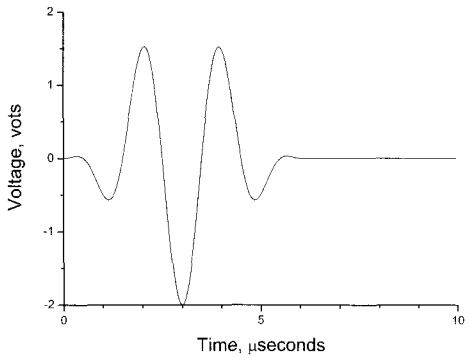

(a)

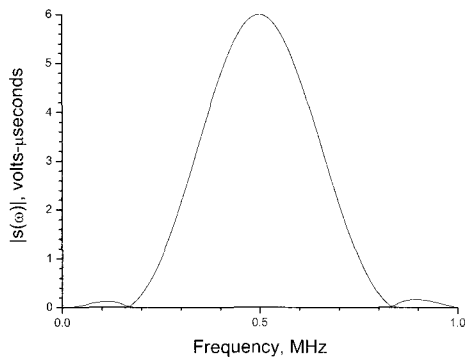

(b)

Fig. 3 The system function used in the present study; a) the assumed front surface reflection signal and b) the corresponding system function

3. Prediction of Reflections from Non-Linear Burning Surfaces

To investigate how the non-linear burning distorts the surface echo waveform, we have simulated the reflection signals for four different cases with different burning surface morphology; 1) for a perfectly planar burning surface without any random roughness, 2) for a globally planar burning surface with random roughness, 3) for a perfectly paraboloidal burning surface without any random roughness, and 4) for a globally paraboloidal burning surface with random roughness. The first case is chosen as a reference to investigate the effects of the random roughness (in the second case) and the localized burning (in the third case). And the fourth one is proposed as the most general non-linear burning case in which the burning surface is distorted most severely by the localized burning and the random roughness at the same time.

In the present study, since our current discussion is focused on the effect of surface morphology only (without including the effect of material properties), we make a further simplification on the material property of the couplant and the propellant. It is widely recognized that both the couplant (made of resin) and the propellant (composed of high molecular materials) have large attenuation coefficients for the longitudinal ultrasonic wave at high frequency. And, the ultrasonic measurement model proposed in this study has the capability of considering these attenuations of the couplant and propellant (as can be seen in eqn. (3)). However, in our current calculation, we ignore these attenuations by simply setting the attenuation coefficients ($\alpha_1(\omega)$ and $\alpha_2(\omega)$) to zero.

Fig. 4 shows the simulation result for the first case. As shown in Fig. 4 a), the burning surface is located at z = 62 mm from the transducer, and is perfectly planar without any random roughness. Fig. 4 b) is the frequency spectrum of model calculation by using eqn. (1) and Fig. 4 c) is the corresponding time domain waveform obtained by taking the inverse Fourier transform to the result given in Fig. 4 b). As can be noticed from the result, when the burning surface is perfectly flat, the time domain waveform shows a high amplitude (with

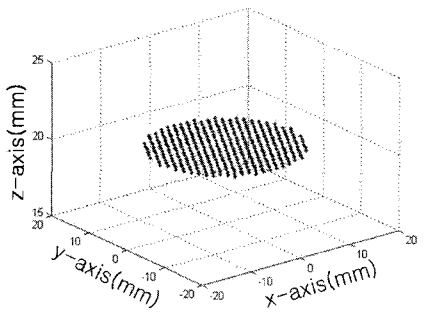

(a)

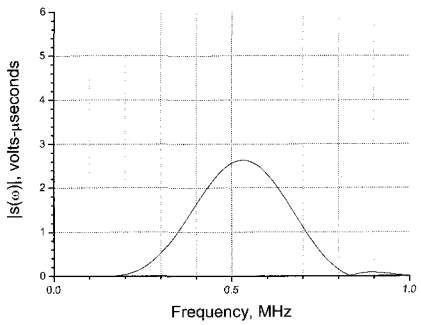

(b)

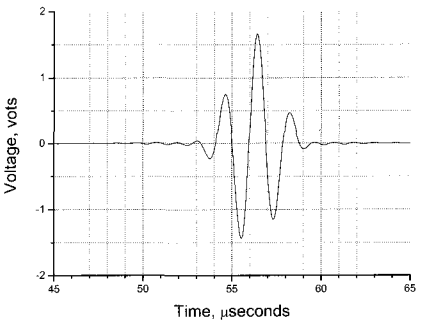

(c)

Fig. 4 Simulation result for the first case, a) a burning surface morphology and b) the predicted frequency spectrum and c) the invoked time domain waveform

the peak-to-peak amplitude of 1.66 volts), and the frequency spectrum has a large peak (about 2.63 volts/MHz) with the peak position at 0.53 MHz.

Fig. 5 summarizes the prediction result for the second case in which the burning surface is

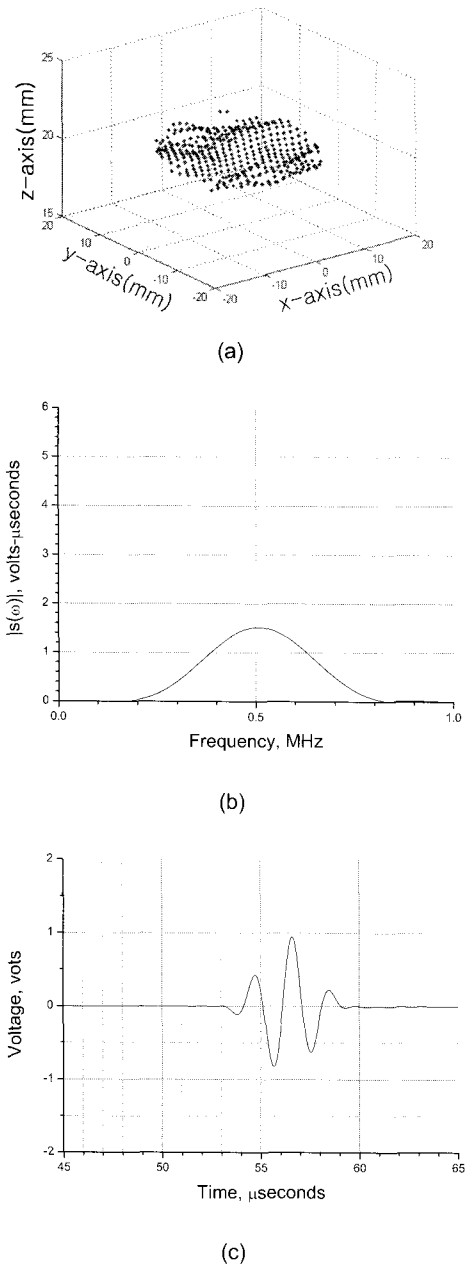

Fig. 5 Simulation result for the second case, a) a burning surface morphology and b) the predicted frequency spectrum and c) the invoked time domain waveform

deteriorated by the random roughness as shown in Fig. 5 a). For the generation of this random rough surface, we have adopted the approach addressed by Ogilvy (1991). For this particular surface, the correlation length (that controls the degree of the randomness) was chosen to be 0.5, and the amplitude (that governs the range of the generated random values) was set to 0.5. As a result, a set of random numbers with a distribution range of -1.0 to 1.0 were generated. Then, these random numbers were added to the z-coordinate values of the small circles in the first case to produce the z-coordinate values of the current random rough surface. Fig. 5 b) and c) show the frequency spectrum and the time domain waveform, respectively, obtained by using the measurement model proposed in the present study. As shown in the figures, the random roughness results in the decreases in the amplitudes of the waveform and the spectrum and the shift of the peak position of the spectrum to 0.02 MHz. However, little change is observed in the time-of-flight of the surface echo, which might be resulted from the smoothing out of the effects caused by the individual elements in an average sense.

Fig. 6 is the result for the third case, where the morphology of the burning surface is in a perfectly smooth paraboloid as shown in Fig. 6 a). The paraboloid is convex to the transducer position so that the incident beam arrives to its central region first. The z-coordinate of the center is 1 mm apart along the z-axis from that of its periphery. To describe such a morphology, the z-coordinates of the small circular elements have been carefully chosen, and the individual elements were moved along the z-axis by proper distances with the normal of the elements fixed along the z-axis. Fig. 6 b) shows the frequency spectrum of the signal reflected from this paraboloidal surface, and Fig. 6 c) is the corresponding time domain waveform. The amplitude of the signal drops almost by 6 dB compared to that of the signal from the flat planar burning surface discussed in the first

case. Furthermore, the peak frequency of the spectrum is shifted by 0.03 MHz compared to the first case. In addition, the arrival time of the surface echo is also shifted due to the change in the distance between the transducer and the burning surface.

Fig. 7 presents the result for the fourth case, where the paraboloidal surface with random roughness. This surface was invoked by superimposing random rough surface created in the second case to the paraboloid generated in the third case. The resulted surface is shown in

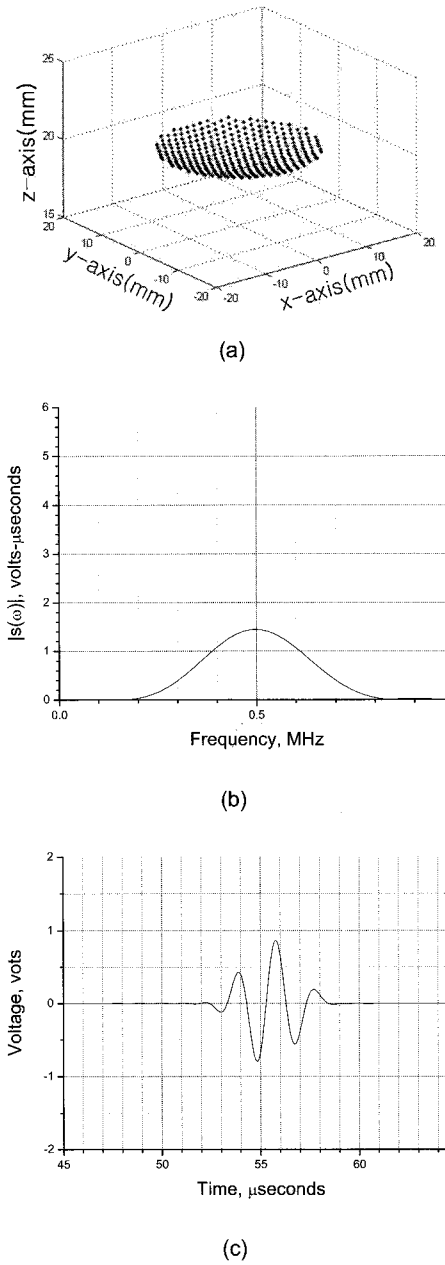

Fig. 6 Simulation result for the third case, a) a burning surface morphology and b) the predicted frequency spectrum and c) the invoked time domain waveform

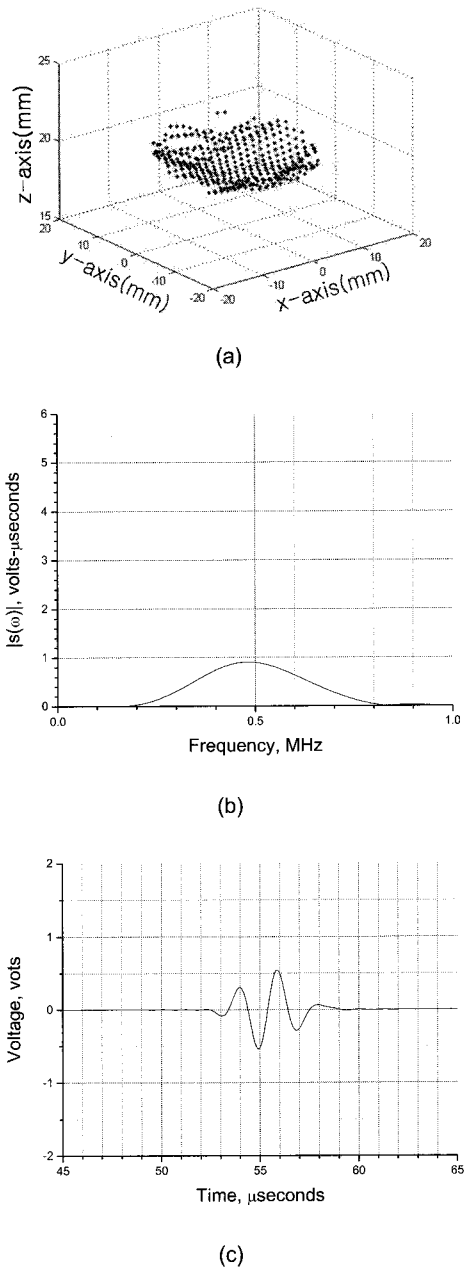

Fig. 7 Simulation result for the fourth case, a) a burning surface morphology and b) the predicted frequency spectrum and c) the invoked time domain waveform

Fig. 7 a). From the results shown in Figs. 7 b) and c), it is easily recognized that the considerable change in the time domain waveform shape and the shift of the peak frequency of the spectrum (by about 0.05 MHz) compared to those of the first case (presented in Figs. 4 b) and c)). Obviously, the amplitude of the signal decreases significantly (by almost 70 % compared to the reference case) and becomes the lowest one among these four cases.

From above simulation, it is clear that the non-linear burning of the propellant can cause the waveform change of the burning surface echo together with the corresponding spectrum variation. Therefore, it should be able to identify the existence of the non-linear burning from the analysis of the waveforms and frequency spectra of the signals acquired during the propellant burning. However, the waveform and frequency spectrum is also influenced by the material property variation as discussed by Oh et al (2007), further investigation is needed to have more sound understanding on this complicated phenomenon.

4. Conclusion

In the present study, we have proposed an ultrasonic measurement model that can predict the reflections from solid propellant surfaces with non-linear burning. Specifically, we have successfully developed the desired model by the combination of two ingredients; 1) a pulse-echo ultrasonic measurement model for a planar, circular reflector imbedded in the second medium in an immersion set-up, and 2) an efficient description of non-linear burning surfaces with a number of small, planar circles.

In the present work, the proposed measurement model has been applied to predict the surface echo signals from four different burning surfaces that have been generated by the combination of two factors; the base shape (flat or paraboloidal) and the surface roughness (perfectly smooth or randomly rough). From the simulation presented here, we have confirmed that the non-linear burning of the propellant can cause the waveform change of the burning surface echo and the corresponding spectrum variation. Therefore, there should be the possibility of identifying the existence of the non-linear burning from the analysis of the waveforms and frequency spectra. However, the waveform and frequency spectrum can also be altered by the material property variation, so that further investigation should be performed to have sound understanding on this complicated phenomenon.

Acknowledgement

The authors would like to thanks to Defense Acquisition Program Administration and Agency for Defense Development for the financial support.

References

Frederick Jr., R. A., Traineau, J-C. and Popo, M. (2000) Review of Ultrasonic Technique for Steady State Burning Rate Measurements - 36th AIAA/ASME/SAE/ASEE Joint Propulsion Conference and Exhibit, AIAA paper 2000-3801, Huntsville, AL

Huang, D. and Breazeale, M. A. (1999) A Gaussian Finite-Element Method for Description of Sound Diffraction, J. Acoust. Soc. Am., 106, pp. 1771-1781

McQuade, W. W., Dauch, F. D., Moser, M. D. and Frederick Jr., R. A. (1998) Determination of the Ultrasonic Burning Rate Technique Resolution - 35th AIAA/ASME/SAE/ASEE Joint Propulsion Conference and Exhibit, AIAA paper 1998-3555, Cleveland, OH

Ogilvy, J. A. (1991) *Theory of Wave Scattering*

from Random Rough Surface, Adam Hilger, Bristol, New Work

Oh, H. T., Kim, H. J., Song, S. J., Ko, S. F., Kim, I. C., Yoo, J. C. and Jung, J. Y. (2007) Investigation of Ultrasonic Methods for Measuring Burning Rates of Solid Propellants, Submitted to Review of Progress in Quantitative Nondestructive Evaluation, AIP, New York

Salvo, R., Frederick Jr., R. A., Moser, M. D. and Cohen, N. S. (1999) Direct Ultrasonic Measurements of Solid Propellant Combustion Transients - 35th AIAA/ASME/SAE/ASEE Joint Propulsion Conference and Exhibit, AIAA pp. 1999-2223, Los Angerles, CA

Schmerr, L. W. (1988) *Fundamentals of Ultrasonic Nondestructive Evaluation – A Modeling Approach*, Plenum, New York

Schmerr, L. W. and Song, S.-J. (2007) Ultrasonic Nondestructive Evaluation Systems – Models and Measurements, Springer, New York

Song, S. J., Jeon, J. H., Kim, H. J., Kim, I. C., Yoo, J. C. and Jung, J. Y. (2006) Burning Rate Measurement of Solid Propellant Using Ultrasonic - Approach and Intial Experiments, Review of Progress in Quantitative Nondestructive Evaluation, Vol. 25B, AIP, New York, pp. 1229-1236

Song, S. J., Kim, H. J., Ko, S. F., Oh, H. T., Kim, I. C., Yoo, J. C. and Jung, J. Y. (2007) Measurement of Solid Propellant Burning Rates by Analysis of Ultrasonic Full Waveforms, Submitted to KSME International

Sutton, G. P. and Biblarz, O. (2001) Rocket Propulsion Elements, Wiley-Interscience Publication 7th Ed., New York, pp. 417-430